# Study of Currents and Temperature of Induced Spur Gear using 2d Simulation

N. Barka, P. Bocher, A. Chebak, J. Brousseau and D. S. Ramdenee

*Abstract*—This paper presents the study of induced currents and temperature distribution in gear heated by induction process using 2D finite element (FE) model. The model is developed by coupling Maxwell and heat transfer equations into a multi-physics model. The obtained results allow comparing the medium frequency (MF) and high frequency (HF) cases and the effect of machine parameters on the evolution of induced currents and temperature during heating. The sensitivity study of the temperature profile is conducted and the case hardness is predicted using the final temperature profile. These results are validated using tests and give a good understanding of phenomena during heating process.

*Keywords*—2D model, induction heating, spur gear, induced currents, experimental validation

## I. Introduction

THE sensitivity study of the hardness profile conducted for sample geometry such as the disks based on axisymmetric 2D models cannot be reused for complex geometries. The results can be very useful for the development of simple parts, but they can never be applied to complex geometries such as gears or splines. It is then necessary to develop a 2D model that can demonstrate the same effects for the gears and converging towards a model able to predict the hardness profile as a function of machine parameters [1-3].

During the process development of various spur gear geometries, it is some time difficult to achieve the required hardness profile. In fact, it seems that the medium frequency is not always capable of concentrating the heat at the root. Generally, to achieve the desired hardness profile in a gear two major concepts are used. The first one, called also sequential heating process, is consisting in applying a medium frequency (MF) flash which is supposed to distribute heat at the tooth root, followed by a high frequency (HF) flash to austenitize the part and generate the hardness profile upon quenching. The second concept consists in a single heating step, applying simultaneously MF and HF flashes to generate heat at the tip and the root [4-6]. Such a scenario seems quite simple, however; based on our experience, the medium and high frequencies generators are not always able to harden correctly all gear geometries with different external diameters.

This paper introduces first, the 2D model, the convergence study conducted to optimize the mesh and the assumptions used in modeling and operation conditions. Second, it discusses sensitivity analysis in case of medium frequency (MF) and high frequency (HF) based on the study of induced currents density and temperatures in the gear. Finally, an experimental study is conducted to validate the models developed and a calibration is performed to determine the power ratios are useful in the both cases MF and HF. These ratios are used to validate the development of recipes using heating combined MF and HF.

N. Barka is mechanical engineering professor at the University of Quebec at Rimouski, 300 allee des Ursulines, Rimouski (Quebec) G5L 3A1 Canada (phone: 418-723-1986 ext 1949; e-mail: noureddine_barka@uqar.qc.ca)

P. Bocher is mechanical engineering professor at the École de technologie supérieure, 1100, rue Notre-Dame Ouest, Montréal (Québec) H3C 1K3 (phone 514-396-8645; e-mail : philippe.bocher@etsmtl.ca)

A. Chebak is electrical engineering professor at the University of Quebec at Rimouski, 300 allee des Ursulines, Rimouski (Quebec) G5L 3A1 Canada (phone: 418-723-1986 ext 1876; e-mail: ahmed_chebak@uqar.qc.ca)

J. Brousseau is dean of undergraduate studies at the University of Quebec at Rimouski, 300 allee des Ursulines, Rimouski (Quebec) G5L 3A1 Canada (phone: 418-723-1986 ext 1541; e-mail: jean_brousseau@uqar.qc.ca)

D. S. Ramdenee is graduate student at the University of Quebec at Rimouski, 300 allee des Ursulines, Rimouski (Quebec) G5L 3A1 Canada (phone: 418-723-1986; e-mail: dreutch@hotmail.com)

## II. 2D Model

### A. Model

A 2D model using the finite element method is used to solve the thermal-electromagnetic coupling and thus determine the temperature distribution in a spur gear made from low-alloy steel (AISI-4340) with $\phi$ 105.2 mm external diameter and 6.5 mm thick and 48 teeth [7]. The 2D model includes a gear tooth represented with angle of 7.5°. The finite element model takes into account the following assumptions (Figure 1). The material is considered homogeneous and isotropic. The initial ambient temperature is set at 293 K (20 °C). Magnetic isolation is imposed at limits (1, 10), (10, 11) and (1, 11). Thermal insulation is imposed at limits (1, 10) and (1, 11). An ambient temperature of 293 K (20 °C) is taxed to the limit (10, 11). The inductor is represented by a solid section of 30 mm thick copper. The model components are surrounded by an environment with a dielectric permeability ($\mu_r = 1$) and a vacuum permittivity ($\varepsilon_r = 1$). The energy lost by convection is assumed equivalent to the energy lost by conduction through the air at the interface room / ambient environment. The energy lost by radiation is neglected because of the short time of treatment [8-9].
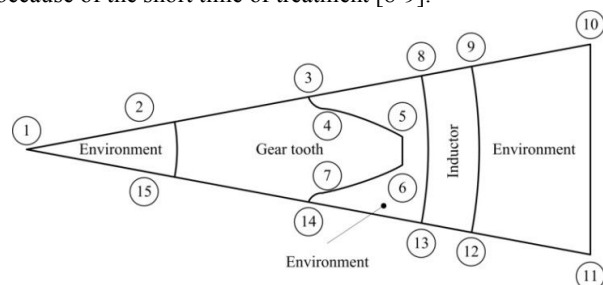


Fig. 1 Schematic representation of the 2D model

### B. Convergence Study

A convergence study was performed on the 2D model and has optimized the mesh according to the induced current density in the inductor and part temperature using the two frequencies (MF and HF). The mesh size is 0.1 mm at the core and are thinner (0.01 mm) at the tooth contour and the inside inductor circumference. The final mesh is showed in Figure 2 and contains 545,000 elements and 1,132,700 degrees of freedom. The imposed current density ($J_0$) is adjusted to have a specific temperature at the gear surface. The two frequencies used are the medium frequency (MF) adjusted at 10 kHz and high frequency (HF) in the range of 200 kHz.
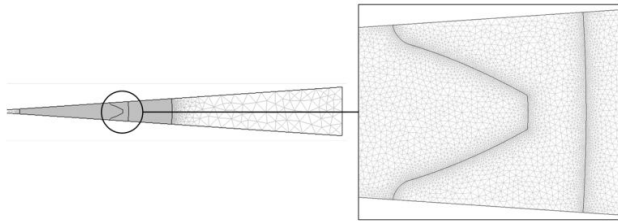


Fig. 2 Optimal mesh used in simulation

### III. COMPARISON BETWEEN MF AND HF

Before studying the effect of the imposed current density and heating time on the hardness profile, it is important first to compare the two MF and HF cases based on the distributions of induced currents density and temperature. For this study, the heating time is set at 0.50 s and $J_0$ in the inductor is adjusted to $2.5 \times 10^9$ A.m$^{-2}$ for MF and $8.1 \times 10^9$ A.m$^{-2}$ in the HF case to reach 1000 °C. The first simulation results are presented in Figures 3 and 4 and can confirm that in the case MF, currents are distributed profoundly in the inductor and the tooth. However, the induced current density is much greater at the tooth root; therefore, they generate more heat in this region where the temperature reaches about 1000 °C, while the temperature in the region of the head the tooth not exceeding 700 °C. In the HF case, the currents are distributed along the tooth contour, but they generate much more heat in the tip and and pitch diameter regions than at the root. Consequently, the heat generated heats the tip at about 1000 °C and the pitch diameter to over 900 °C while the temperature in the root region doesn't exceed 600 °C.
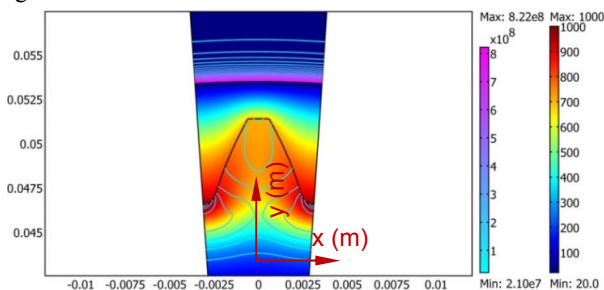
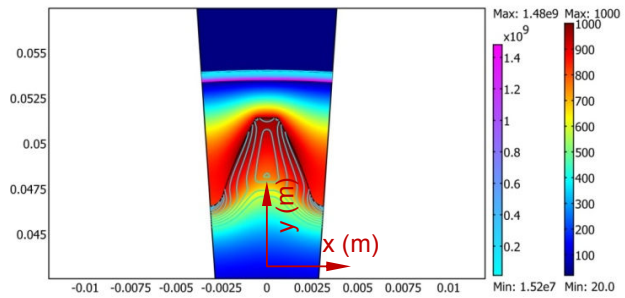

Fig. 3 Distributions of induced currents (A.m$^{-2}$) and temperature (°C) - MF



Fig. 4 Distributions of induced currents (A.m$^{-2}$) and temperature (°C) - HF

These preliminary results allow drawing conclusions from the final temperature distribution in gear and their impact on the obtained hardness profile. The simulation confirms that in the MF case, the area around the tooth root is transformed into martensite, while in the HF case, the tip region and the adjacent side is hardened. Simulation efforts allow also estimating the RMS current applied in the inductor and the power received by gear during the heating. The mean currents are respectively of about 7.4 kA in the MF case and about 2.8 kA in the HF case. The average thermal power consumed by the gear is about 64 kW (MF) and about 50 kW (HF). The results obtained allowed to distinguish the behavior of each MF and HF heating and permit to understand the relationship between the total current density and temperature in the gear. However, material properties, which depend on the heating temperature, affect the magnetic field and temperature distribution. It is then necessary to carefully analyze the total current density and temperature to better understand their evolution during heating.

### IV. STUDY OF INDUCED CURRENTS DENSITY

The study of the induced currents densities at the tip and root of the tooth in both MF and HF can explain clearly how the frequency affects the process and how these currents vary with heating time for the same operation conditions. Figures 5 and 6 show the distribution of the induced current densities versus depth and heating time at the tip and the root of the tooth. At the tip, the induced currents density has a maximum surface value about $6 \times 10^8$ A.m$^{-2}$ and decreases exponentially with depth at the heating start. After 0.2 second, the maximum surface value becomes much lower and decreases slightly with depth. It should be noted at the heating end, the induced currents density is greater in depth compared to surface as this region is affected by the induced currents values much higher at the root. Precisely, at this location, the induced currents density recorded a maximum surface around $8 \times 10^8$ A.m$^{-2}$ at the heating start and the currents are concentrated at a lower depth compared to the tip region. After 0.3 s, the current density reaches a maximum value of $4 \times 10^8$ Am$^{-2}$ and decreases exponentially with depth. At the heating end, the currents density recorded a maximum total surface and its evolution is disturbed due to the material properties.
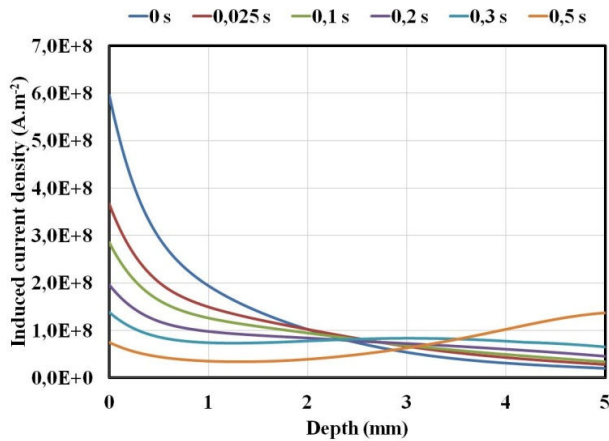
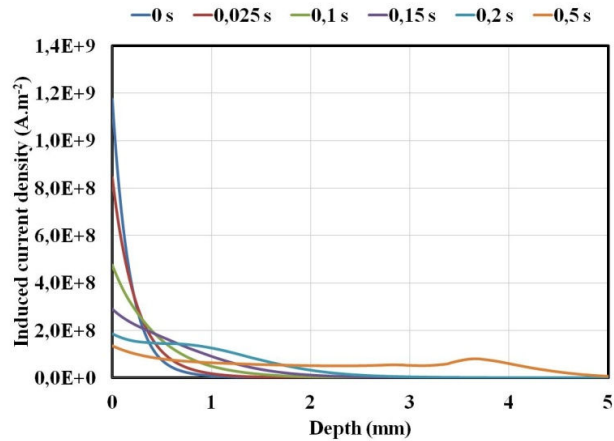Fig. 5 Induced currents density versus depth at the tip (MF)



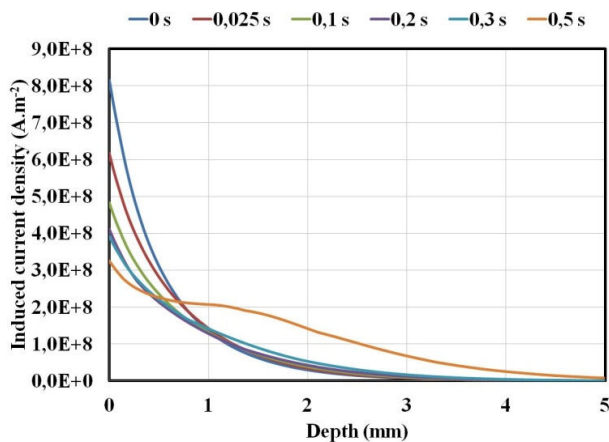Fig. 7 Induced currents density versus depth at the tip (HF)



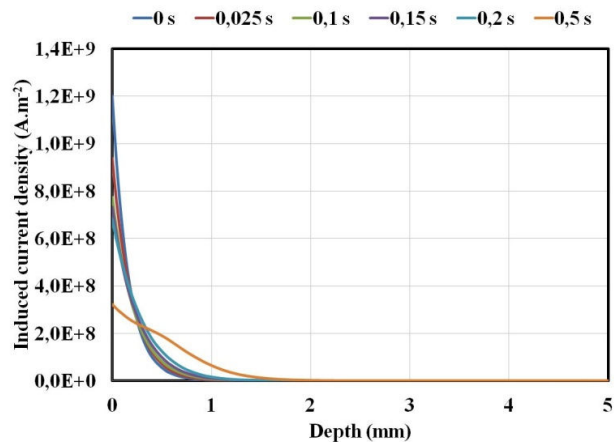Fig. 6 Induced currents density versus depth at the root (MF)



Fig. 8 Induced currents density versus depth at the root (HF)

In the HF case, the currents are concentrated at the heating start at a very shallow depth at the tooth tip (Figure 7). After 0.1 s, the induced currents density is twice lower at the surface. In addition, the value of the surface currents density ($1.2 \times 10^9$ A.m$^{-2}$) passes to $2 \times 10^8$ A.m$^{-2}$ at the heating end. At the root (Figure 8), the currents density has the same magnitude as at the tip ($1.2 \times 10^9$ A.m$^{-2}$) and the currents are concentrated in a shallow depth. The results show that the distribution of induced currents is influenced by changes in material properties. Generally, the induced currents exhibit exponential distributions at the heating beginning with maximum values at the surface. However, by slightly increasing the heating time, the density of induced current behaves differently and the values decrease rapidly at the surface.

## V. STUDY OF TEMPERATURE DISTRIBUTION

The temperature distribution is a consequence of the heat created by the currents induced in the teeth. Figures 9 and 10 respectively show the temperatures at the tip and the root. At the tip, the temperature reaches about 600 °C at the surface after 0.3 s of heating and does not exceed 740 °C at the surface at the heating end. This temperature remains almost constant over a certain depth before declining by going deep. At the root level, temperatures are highest at the surface and decrease rapidly in going to the gear core. At the heating end, the temperature reaches 1000 °C and the surface does not exceed 100 °C to 5 mm deep. Comparing the temperature curves of the two positions shows that the temperature is distributed deeply into the tooth and the temperature remains almost constant over a large depth at the tip while it is concentrated in a shallow root. In addition, the gap between the surface temperatures at the tip and the root is about 300 °C at the heating end. Therefore, the austenitic transformation begins in the tooth root region. The final profile of temperature has a direct effect on the hardness profile obtained and their evolution as a function of depth. While the assumption that all regions heated above the $Ac_3$ temperature

become hard martensite upon cooling is satisfactory and that this temperature is estimated at 850 °C for heating rates involved, it is possible to appreciate the case depth. The obtained results demonstrate that only the tooth root is transformed and the case depth is 0.6 mm in MF case. Finally, a sensitivity study shows that an offset in terms of the temperature curve at the heating end (Figure 10) ± 50 °C around the value 850 °C can be caused by a variation of the imposed current density around the value $2.5 \times 10^9$ A.m$^{-2}$ leads to a depth variation of about ± 0.2 mm around 0.6 mm for MF.
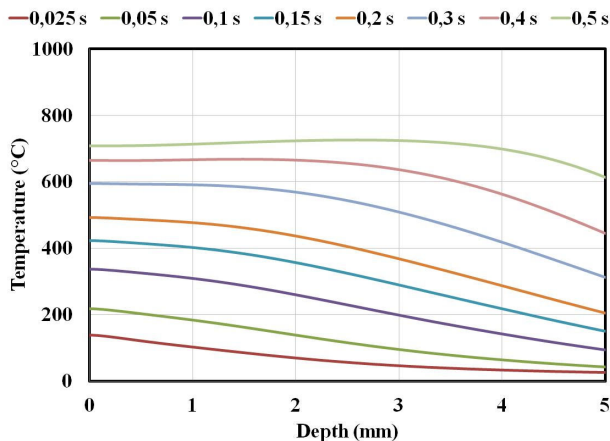


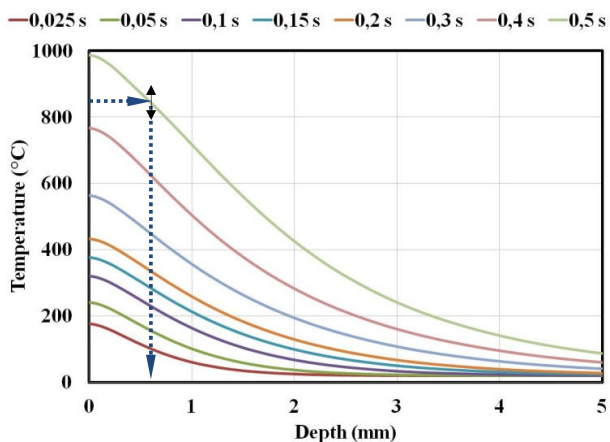Fig. 9 Temperature versus depth at the tip (MF)



Fig. 10 Temperature versus depth at the root (MF)

At the tooth tip (Figure 11), the temperature is concentrated in a shallow near-surface and in the range of 600 °C after only 0.1 s and then reaches 760 °C after 0.2 s before reaching 960 °C at the heating end. At this point, the temperature is distributed over a large depth. At the tooth root (Figure 12), the temperature is 320 °C after 0.1 s of heating. Second, it increases rapidly to 570 °C after 0.3 s of heating. At the heating end, the temperature does not exceed 810 °C and is spread over a shallow depth. Indeed, heat is created following the contour of the teeth at the start of the heater before being concentrated at the tip since the volume to be heated is low.

Once the high temperatures are reached, more heat is created at the tooth root, which heats the tooth side and the middle of the tooth. Figure 11 shows that only the tip region is transformed into austenite and hardened states that the case depth is about 2.1 mm at the tooth tip. The same variation of the temperature curve at the heating end can be caused by a variation of $J_0$ around the value $8.1 \times 10^9$ A.m$^{-2}$ (Figure 11) leads to a variation of ± 0.8 mm depth of around 2.1 mm for HF.
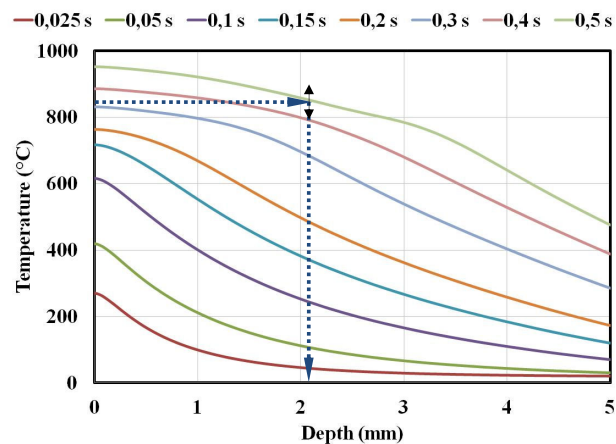


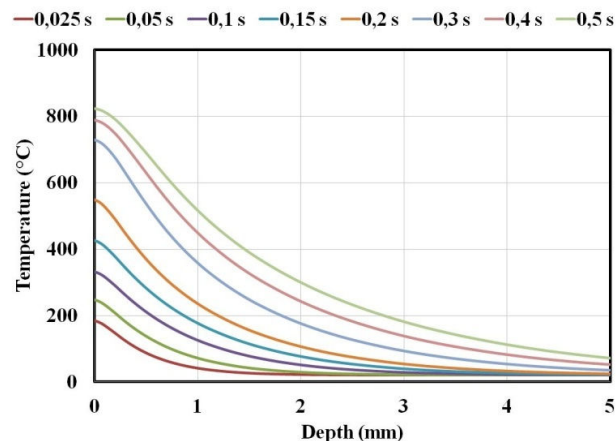Fig. 11 Temperature versus depth at the tip (HF)



Fig. 12 Temperature versus depth at the root (HF)

The surface temperature is a relevant criterion for a first comparison because it is a consequence of the power transmitted to the gear. At this point, it is also interesting to note that the effects are very different compared to the case of induction heating of a hard disk where depths were less sensitive in the HF case compared to MF case.

## VI. EXPERIMENTAL VALIDATION

To validate the simulations, experimental tests were performed on the machine induction heater located at the École de Technologie Supérieure using the same experimental setup presented in previous publications [10]. Several

hypotheses have been considered in this study, in fact, the time between the heating and the shower is neglected, the error of repeatability and setting accuracy due to the machine parameters is considered negligible and the part is centered horizontally and vertically in the inductor. Table 1 summarizes two tests used for this preliminary experimental validation. The case depths are obtained at middle plane and are compared with those obtained by simulation.

TABLE I
VALIDATION EXPERIMENTS

| Test | Frequency (kHz) | Heating time (s) | Power (kW) | Case depth (mm) | | |
|---|---|---|---|---|---|---|
| | | | | Tip | Pitch | Root |
| 1 | 10 | 0.50 | 220 | 0 | 0 | 1.1 |
| 2 | 200 | 0.50 | 83 | 1.5 | 0.3 | 0 |

Initially, only two tests were performed with heating time of 0.50 s and MF and HF cases. The machine powers were increased until a case depth around 1 mm at the root (MF) and about 1.50 mm at the tip (HF). The experimental results were compared using the simulation results that seems an interesting tool to distinguish the regions heated by induction. Using the assumption that any region heated up to the value $Ac_3$ becomes austenite and transforms into martensite upon cooling; it is possible to predict the hardness profile. Thus, the simulation results show that only the root region and a small region around are transformed into hard martensite (Figure 13.a) when the medium frequency is applied (MF). However, if HF is employed, only the tip region and a small area close to the pitch diameter hardened (Figure 13.b). Figure 14 confirms a significant correlation between the simulation results and the experiments in both MF and HF cases.
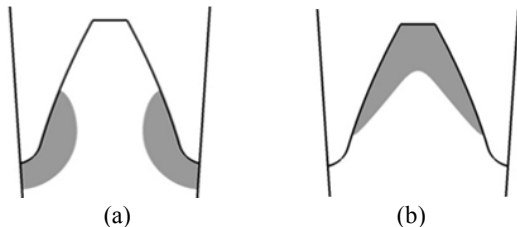


(a)                    (b)

Fig. 13 Hardness profiles obtained by simulation, (a) 10 kHz, 0.50 s et $2.4 \times 10^{10}$ A.m$^{-2}$ et (b) 200 kHz, 0.50 s et $10.7 \times 10^{10}$ A.m$^{-2}$
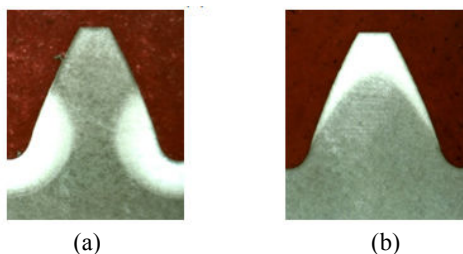


(a)                    (b)

Fig. 14 Hardness profiles obtained by experiments, (a) 10 kHz, 0.50 s et 220 kW et (b) 200 kHz, 0.50 s et 83 kW [10]

The simulation results are consistent with the experimental validation for both tests. However, numerical models can be used to predict the profiles of hardness without establishing the relationship between the parameters of simulation and experimentation, that is, between the imposed current density in the inductor ($J_0$) and power machine ($P_M$). First, it is legitimate to adjust $J_0$ in the inductor in order to have the same hardness profiles in simulation as experiments. Then, a ratio between the machine power ($P_M$) and the power consumed by the gear ($P_S$) could be determined. These results are used to determine roughly hardness profile shape and to analyze the sensitivity of the hardness curve in function of machine parameters variation without additional experimental tests.

Table 2 provides values of power ratio for the two tests used in the previous section. The ratio is more important for HF (67%) compared with MF cases (39%). Both ratios are much lower in comparison to the ratios determined in the case of the disc using the 2D axisymmetric model. This difference can be explained by the fact that the 2D model applied to a gear tooth does not consider the edge effect. Therefore, the calibration of 2D models underestimates the power ratios.

TABLE II
POWER RATIOS

| Test | $P_M$ (kW) | $P_S$ (kW) | Ratio |
|---|---|---|---|
| 1 (MF) | 220 | 85 | 0.39 |
| 2 (HF) | 83 | 56 | 0.67 |

## VII. SUMMARY

This paper has focused on the study of induced currents and temperature according to the machine parameters using a 2D model. First, it presented a 2D model to establish the distributions of the induced current and temperature in a gear made from steel AISI-4340 by optimizing the mesh through a study of convergence and taking into account the simulation parameters and simplifying assumptions. Then, a sensitivity study was conducted to compare the two cases of MF and HF and heating in order to understand the effect of changes in material properties and the relationship between the induced currents and temperatures during the heating. Then, a global sensitivity analysis was used to study the effects of heating time and the imposed current density on surface temperatures and case depth. Finally, it presented the stages of experimental validation and calibration models using the two modes of heating mono-frequency heating.

The parametric sensitivity analysis was used to compare the two cases of MF and HF heating and decide that the 2D models give similar results to those obtained during experimental tests found in the literature [3]. In addition, analysis of induced currents and temperatures showed that the MF power distribute the currents deeply in the part and concentrate them at the root, while the HF power tends to focus the induced currents following the contour. These currents are also affected by the material properties and decreases greatly with the decrease in the relative magnetic permeability and electrical conductivity. Temperatures in the

root region are greater at a shallow depth from the tip region where temperatures are almost constant over the entire height of the tooth. The experimental validation was used to determine ratios of powers by superimposing the hardness profiles obtained experimentally and that got by simulation in the absence of reliable tools for measuring the current flowing through the inductor and the surface temperature. These ratios have been used advantageously in simulation to verify the results of experimental tests obtained using recipes for development on the induction machine.

REFERENCES

[1]  Barka N., Bocher P., Brousseau J., Galopin M., Sundararajan (2007) Modeling and Sensitivity Study of the Induction Hardening Process. Advanced Materials Research, 15-17:525-530.
[2]  Barka N., Bocher P., Brousseau J., Galopin M., Sundararajan., Sensitivity study of induction Hardening machine parameters, 3rd International Symposium on Aerospace Materials and Manufacturing Processes, Montreal, Canada, 2006, pp.781-790.
[3]  Rudnev V., Loveless D., Cook R., Black M., Handbook of Induction Heating, Marcell Dekker Inc., New York, 2003.
[4]  Zinn S., Elements of Induction Heating: Design, Control, and Applications, ASM International, Metals Park, OH, 1988.
[5]  Kawagushi H., Enokizono M., Todaka T., Thermal and magnetic field analysis of induction heating problems, Materials Processing Technology, vol. 161 (2005) 193-198.
[6]  Hammond M., Simultaneous Dual-Frequency Gear Hardening, Electroheat Technologies LLC, 2001.
[7]  U.S. Defense Departement, Metallic Materials and Elements for Aerospace Vehicle Structures, Military Handbook - MIL-HDBK-5H, 1998.
[8]  Haimbaugh R.E., Practical Induction Heat Treating, ASM International, Materials Park, OH, 2001.
[9]  Yuan J., Kang J., Rong Y., Sisson R.D.Jr., FEM modeling of induction hardening process in steel, Worcester polytechnic institute, MA, 2003.
[10] Barka, N, Bocher, P, Brousseau, J, Arkinson, P, Effect of dimensional variation on induction process parameters using 2D simulation, International Conference on Processing and Manufacturing of Advanced Materials, August 2011, Quebec, Canada.